

Exploring the Earth

NORSAR Scientific Report No.1-2014

Semiannual Technical Summary

1 January – 30 June 2014

Tormod Kværna (Ed.)

Kjeller, December 2014

NORSAR

6.2 The modernized large-aperture broadband array NOA

6.2.1 Introduction

The NORSAR seismic array NOA has been operational since 1970. Originally it consisted of 22 sub-arrays with 132 borehole sites and 22 vault sites distributed over an area with approximately 120 km diameter. The borehole sites were equipped with HS-10 vertical short-period seismometers and the vault sites with Teledyne Geotech 8700 three-component long-period sensors, and data were recorded with Philco-Ford 8 bit gain-ranged digitizers. In 1976 the size of the array was reduced to 7 subarrays (42 HS-10 and 7 Teledyne-Geotech 8700) and in 1994 the Philco-Ford digitizers were replaced by Nanometrics RD6 digitizers. A major refurbishment was conducted in 1994-1995 by installing new sensors (42 Teledyne Geotech 20171 short-period and 7 Teledyne Geotech KS54000 borehole broadband sensors) and digitizers (Science Horizons AIM24) at all sites. In year 2000 one of the KS54000 was replaced by a Güralp CMG-3T in order to comply with the CTBTO requirements for certification as IMS station, but otherwise the configuration was unchanged until 2011.

The planning for the latest modernization/recapitalization of the NORSAR array in 2011 started already in 2006. The equipment became obsolete/outdated and was not supported anymore by the manufacturer. The proper operation of the array was at risk due to the lack of spare parts. It took about 2 – 3 years to obtain the necessary funding for the refurbishment of the complete NOA array (jointly financed by CTBTO and Norwegian Ministry of Foreign Affairs). Equipment specification, procurement, prototype testing and several rounds of prototype revisions required another 2 years. The installation of the new equipment was distributed over half a year, with one subarray completed at any time, so that the IDC could retain station NOA in operations with reduced configuration, while testing the new configuration in a testbed. On July 5, 2012, the last site of the NOA array had been upgraded.

The continuous operation of the NORSAR array through more than 40 years provides a unique archive of historic seismological data of nuclear explosions, earthquakes, natural and man-made events. For the years 1971-1983, events were selected for archiving, but after 1983 all continuous data are archived. All available data for the complete time period are online, easy accessible on disk and open to the public.

6.2.2 Location and infrastructure

The NOA array has a diameter of about 60 km and its 42 sites are arranged in 7 sub-arrays (NAO, NBO, NB2, NC2, NC3, NC4, NC6) with sub-array diameters of 6 – 8 km and 6 sites each (Figure 6.2.1). Each sub-array has 5 borehole sites (BH), one vault site (VS) and a central terminal vault (CTV) with power and communication (the vault sites and the borehole sites were earlier called long-period vaults and short-period sites, respectively, but this is somewhat misleading now, because after the upgrade all sites are equipped with broadband instruments). The power system in the CTVs receives power from the public grid and charges a UPS with a battery bank providing about 3 days operation capacity for the entire sub-array. Each site of the sub-array is individually connected by a single cable with the CTV. These cables (some of them as long as 14 km) provide DC-power as well as communication to the sites. In total the array has about 155 km of cable trenches, affecting 127 landowners.

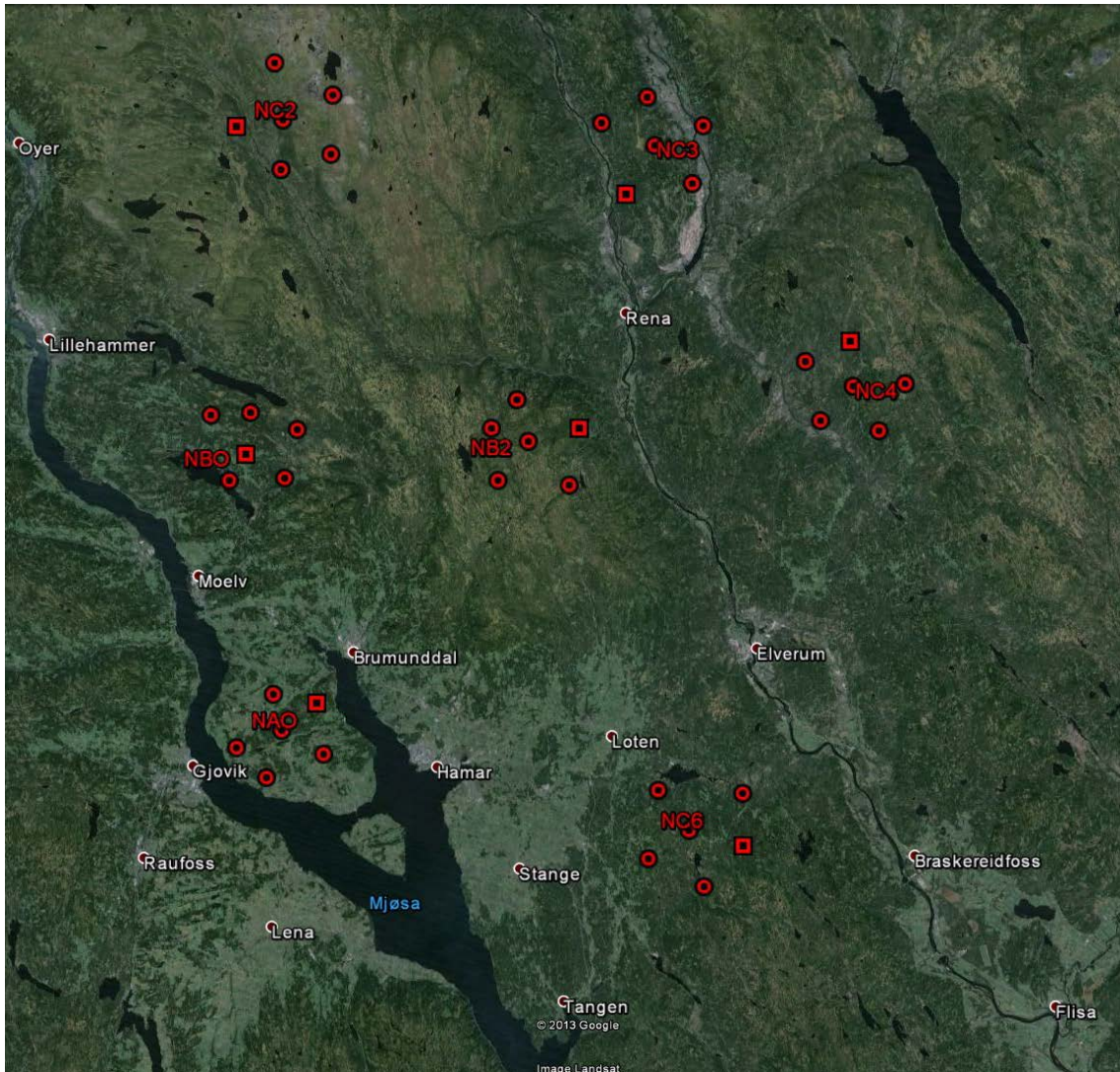


Fig. 6.2.1. Map of the NOA array. Borehole sites are marked with circles, vault sites with adjacent terminal vaults are marked by squares. The yellow line indicates a 20km scale.

Representative for all CTVs, Figure 6.2.2 shows the Central Terminal Vault at sub-array NAO. The picture was taken in 2012 during the migration to a new VSAT technology and the repointing of the satellite dishes. Originally the CTVs did not have the small superstructure, which was cumbersome in wintertime since then the door of the actual vault opened upwards and the snow height can easily reach 2 meters. The picture on the right hand side shows the equipment inside of the CTV, i.e., the rack with modems and lightning protection cards, the power distribution box, the UPS and the battery rack. From the CTV, 48 V DC is distributed to the 6 sites. The communication is established by modems and PPP-protocol. Due to the long-distance cables our transmission rate is limited to 38400 bit/s (19200 bit/s for the most remote site).

Figure 6.2.3 shows the entrance and the interior of the vault site at NC6. Only one of the three pits is used for the regular operation the remaining pits are free for instrument testing. An example of a borehole site is given in Figure 6.2.4. Under normal conditions only the GPS mast and the lid of the site is visible. The digitizer and the pit boxes are installed in a drum on top of the borehole. The sensor is down on the bottom of the borehole securely locked to the borehole wall with a clamping mechanism.



Fig. 6.2.2. Central Terminal Vault (CVT) at NAO. In 2012 NORSAR migrated to new VSAT technology and the antenna dish needed to be pointed to a new satellite. Right: Inside of the CVT. From left to right: rack with modems and power distribution to pits, cable box to pits with coarse lightning protection, and uninterruptable power system with battery rack.



Fig. 6.2.3. Vault site (VS) at NC6. The VSs have 3 pits (formerly used for the 3 components of long-period sensors). With the current installation only one of the pits is used.



Fig. 6.2.4. Borehole site (BS) NC601. The sensor is installed in a shallow (down to 12 m depth) borehole. A zinc drum on top of the borehole contains the digitizer (Güralp CMG-DM24S3EAM), a power and communication pit box (lightning protection, battery power charger, Patton modem, 12V 800mAh battery bank) and a junction box (coarse lightning protection and 48/12 DC/DC converter).

6.2.3 Instrumentation

The recapitalization of the NOA array comprised new acquisition computers for the 7 CTVs, modified pit boxes, new digitizers and new sensors; the communication/power cables, UPSs, vaults and boreholes were not included in this upgrade (but are maintained on a regular basis).

All sites are equipped with Güralp CMG_DM24S3AM acquisition modules. These allow for remote control of the sensors (lock, unlock, center, calibrate, etc.), state-of-health and tamper monitoring, local data storage (set up for a 14-days buffer), data signing and realtime data transmission to the CTV.

The decision to install Güralp seismometers, with a hybrid instrument response, was made after careful analysis of the noise conditions on all our arrays (NOA, ARCES and SPITS), the experiences with the existing systems and the need to have a good monitoring capability for both regional high-frequency/low-magnitude events as well as global low-frequency/high-magnitude earthquakes. Furthermore, the intention was to use this type of instrument also for the later recapitalization of the ARCES array. The hybrid response function was specified by NORSAR and engineered by Güralp. This process involved comprehensive testing of the instruments (but also of the digitizers) and adjustments (e.g., Roth et al. 2011). Table 6.2.1 contains the system responses of the two new sensor types: (i) for the 3-component very-broadband sensor (CMG-3T Hybrid 360s – 50Hz) in a surface-mount casing and (ii) for the vertical-component broadband sensor (CMG-3V 120s – 50 Hz) in a

borehole casing. The seven vault sites of NOA have been equipped with the 3-component sensor and the 35 borehole sites have been equipped with the vertical-component sensor. The transfer functions for both models are identical for frequencies above 0.2 Hz (see Figure 6.2.6), which allows array processing of all data for that frequency range without instrument correction. For frequencies above 0.01 Hz the amplitude response is identical and only the phase response differs. However, array processing tests with long period data show that these phase response differences can be neglected for frequencies above 0.02 Hz.

CMG-3T Hybrid 360s - 50Hz		CMG 3V Hybrid 120s – 50 Hz	
2x20000 V/m/s @ 5Hz		2x20000 V/m/s @ 5Hz	
3 Zeroes	7 Poles	3 Zeroes	7 Poles
0	-2	0	-2
0	-1.964E-3+1.964E-3j	0	-5.89E-3+5.89E-3j
-0.3333	-24+21j	-0.3333	-24+21j
	-41+114j		-41+114j

Table 6.2.1. Poles and zeroes (in units of Hz) defining the velocity response of the hybrid sensors.

Figure 6.2.5 shows instrument responses for a variety of NORSAR installations (for a complete overview see Pirli, 2013). Two short-period systems (the Teledyne instruments formerly installed in the NOA borehole sites and the GS13 sensors of the NORES array), two broad-band systems proportional to acceleration (the KS54000 formerly installed in the NOA vault sites and Gralp 3T of the SPITS array), four broad-band systems proportional to velocity and the two new broad-band systems with hybrid response (bold, dashed lines). The absolute levels of the hybrid systems match the levels of the short-period systems, the SPITS and NOA broadband systems for a frequency of about 5 Hz.

Figure 6.2.6 compares the former NOA instrumentation with the new one. The plots show the velocity responses in order to highlight the 2 different plateaus of the hybrid response. The new systems are proportional to velocity for frequencies from 0.01Hz (0.005Hz) to about 0.2Hz and for frequencies between 3 – 20Hz. In the intermediate range, the instruments are proportional to acceleration. Traditionally, sensors are either proportional to ground velocity or to ground acceleration. The new sensor type is both and therefore its name ‘hybrid’. The advantage of the hybrid sensor is its ability to record weak regional/local high-frequency events with sufficient gain as well as strong earthquakes in regional/global distances. A velocity-proportional sensor adjusted for weak high-frequency events would clip for signals of large magnitude earthquakes in regional/global distances (as observed for instance for our broad-band sensor at ARCES (see Figure 6.2.5). On the other hand, a velocity-proportional sensor adjusted for the monitoring of regional/global earthquakes, would not have enough gain to properly monitor high-frequency explosions at regional distances, which are of interest.

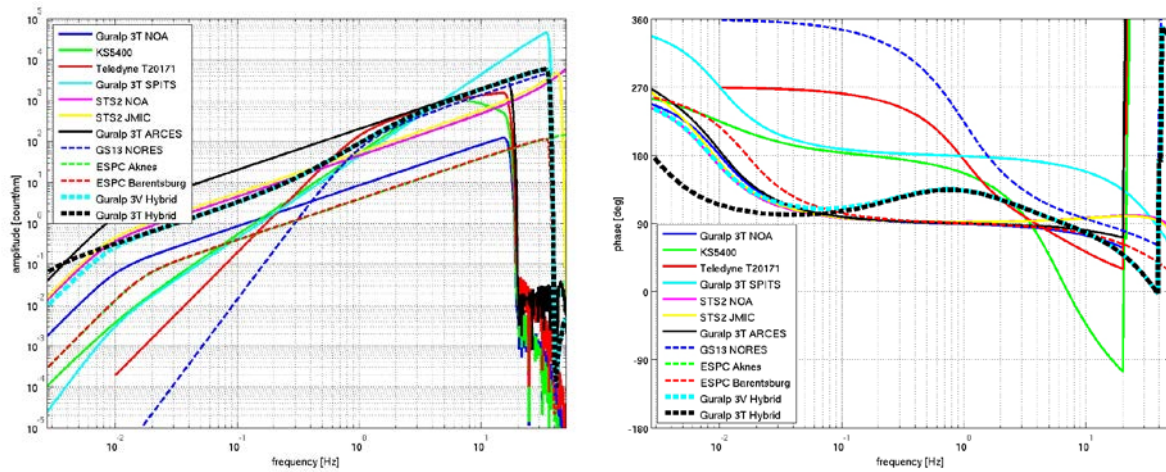


Fig. 6.2.5. System responses of various NORSAR installations. Left: Displacement amplitude response, right: phase response.

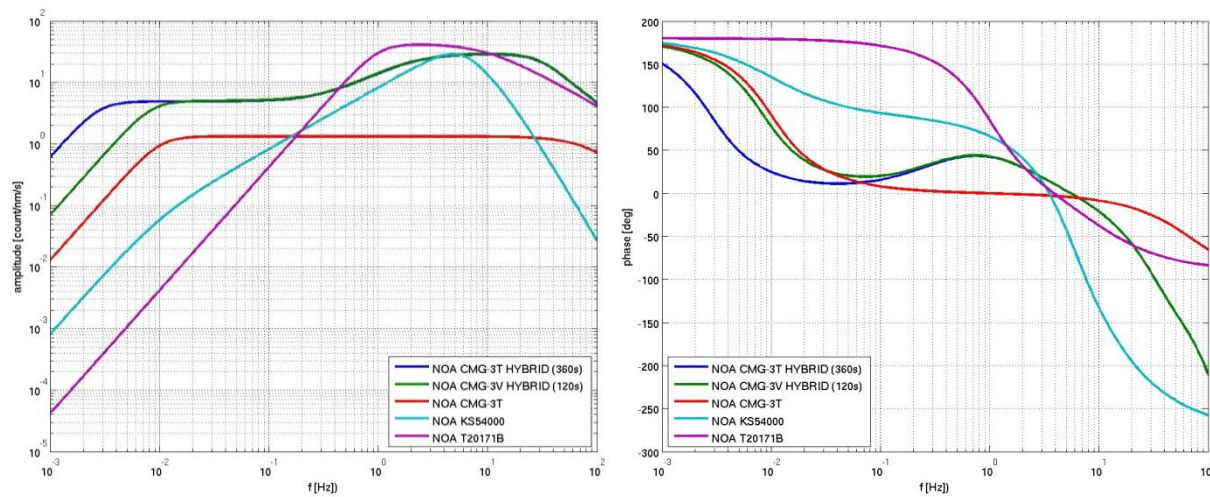


Fig. 6.2.6. System responses of the old (CMG-3T, KS54000, T20171B) and new NOA instrumentation (CMG 3T Hybrid (360s), CMG 3V Hybrid (120s)). Left: Velocity instrument responses, right: phase responses.

Figure 6.2.7 (left) shows the setup for coherency tests for the CMG 3V borehole sensors in the basement of our field laboratory in Hamar. Two prototype instruments had been tested thoroughly for a longer time period in our facility at Stendammen. This was not possible for the major bulk of the instruments, but all of them were checked with respect to instrument noise, mass drift, temperature dependency, waveform coherency, etc. for at least several days at our field lab. The picture on the right hand side of Figure 6.2.7 shows a borehole sensor with mounted hole lock just before deployment. The sensors are lowered to the bottom of the boreholes (8 – 12m deep) and locked to ensure good coupling. In addition, a rubber foam plug was installed in the borehole close to the top of the instrument. The plug minimizes the air volume around the sensor and therefore decreases noise due to thermal convection. Figure 6.2.8 shows an opened Gralp 3T Hybrid sensor and on the right hand side the pit where it was eventually installed. Like for the borehole installations a good thermal insulation helps to avoid long-period noise due to air convection around the sensor.



Fig. 6.2.7. Güralp CMG-3V Hybrid borehole sensors. Left: Test setup, right: just before installation with hole lock attached.



Fig. 6.2.8. Güralp CMG-3T HYBRID sensor. Left: Cover removed, right: installed in one of the vault pits. The sensor is covered with an insulation tube.

The deployment of the sensors and digitizers was done in several stages. In June 2011, the 3-component instruments were deployed (CMG-3T HYBRID) into the 7 vault sites and the obsolete equipment (6 KS54000 sensors, 1 CMG-3T standard, 7 Nanometrics digitizers) were removed. The original 42 short-period instruments remained in place (35 borehole sites and 7 vault sites) for the time being, because the CMG-3V borehole instruments were still in a test phase mainly with issues of mass drift. In September 2011, the decision was made NOT to start with the upgrade of all sites that late in autumn. Early snowfalls could have prevented the completion and then the NOA array would have been difficult to operate during the winter with the mixed instrumentation. However, in October 2011, one of the short-period borehole instruments in each subarray was replaced with a new CMG-3V. This decreased the overall performance of the NOA array (to an acceptable degree), but performance and reliability of the new equipment could be tested in winter conditions. Finally, during the time period April – June 2012, the upgrade of the remaining NOA sites was completed (see Table 6.2.2 for the startup of the sites). The modernized NOA array has been operational since summer 2012.

Site	start	Site	start	Site	start	Site	start
NAO00	15.05.2012	NBO00	20.06.2011	NB200	20.06.2012	NC200	21.06.2012
NAO01	20.06.2011	NBO01	15.08.2012*	NB201	20.06.2011	NC201	27.04.2012.
NAO02	14.05.2012	NBO02	25.08.2012*	NB202	16.06.2012	NC202	14.06.2012
NAO03	25.10.2011	NBO03	25.10.2011	NB203	20.06.2012	NC203	21.10.2011
NAO04	15.05.2012	NBO04	24.05.2012	NB204	19.10.2011	NC204	20.06.2011
NAO05	15.05.2012	NBO05	15.08.2012*	NB205	20.06.2012	NC205	05.07.2012
NC300	14.06.2012	NC400	07.06.2012	NC600	23.05.2012	*) sites were installed but power/communication cables had been damaged during road construction and could not be repaired before August 2012	
NC301	14.10.2011	NC401	14.06.2012	NC601	25.05.2012		
NC302	07.06.2012	NC402	07.06.2012	NC602	20.06.2011		
NC303	20.06.2011	NC403	20.10.2011	NC603	23.05.2012		
NC304	15.06.2012	NC404	14.06.2012	NC604	23.05.2012		
NC305	07.06.2012	NC405	20.06.2011	NC605	25.07.2011		

Table 6.2.2 Startup times of new hybrid sensors at NOA sites (upgrades in 2011 are marked in bold face). The last site was installed 5th July 2012,

Figure 6.2.9 compares the old and new distribution of broadband sensors in the NOA array. Going from 7 to 42 broadband sensors improves the array transfer function especially for long-period signals, e.g., surface waves and provides high channel redundancy.

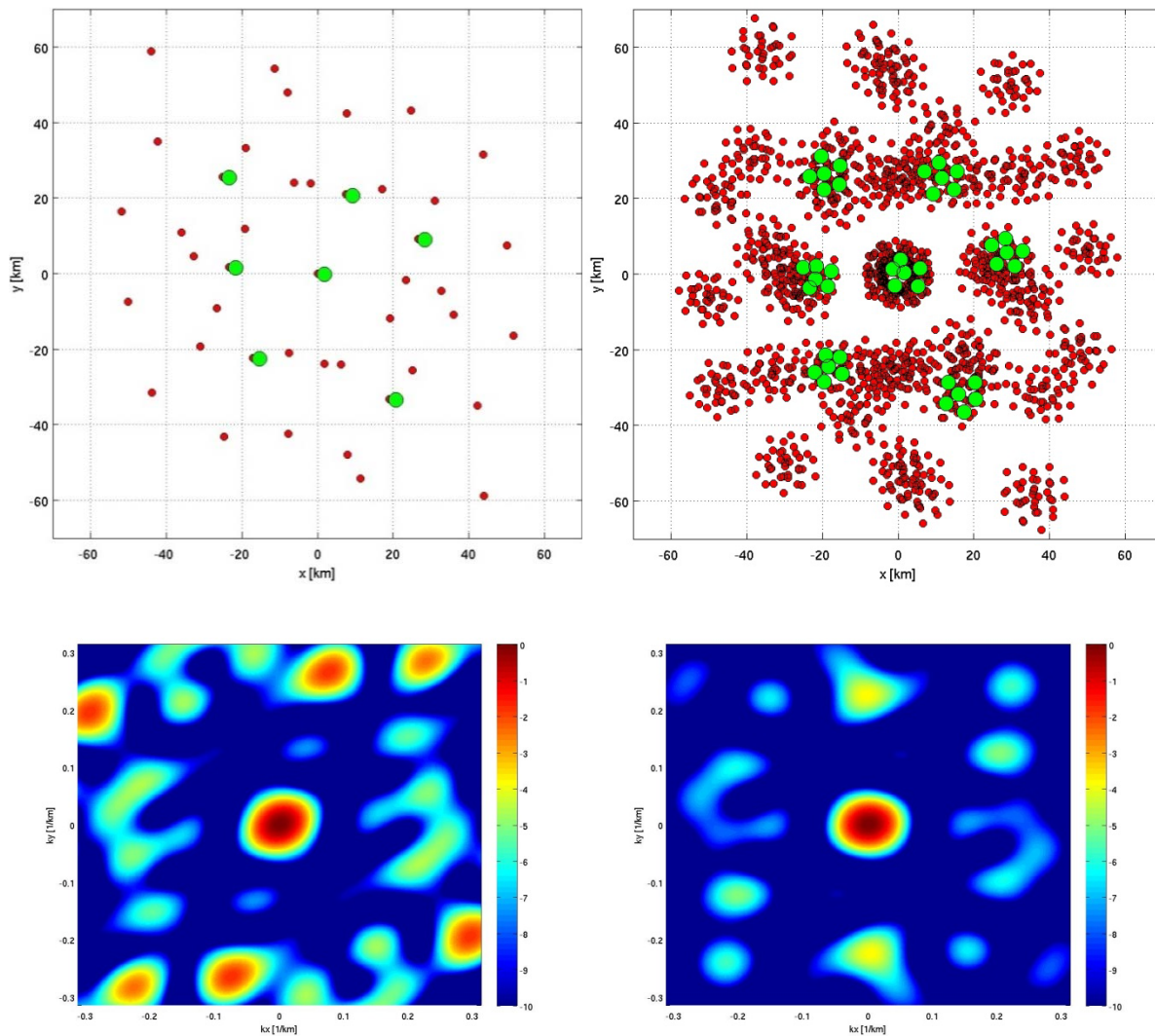


Fig. 6.2.9. Top: Array sites (green dots) and co-array (red dots) for NOA broadband sites. Left: old configuration with 7 broadband sites, Right: new with 42 broadband sites. Bottom: Broadband array response. Left: with the original 7 broadband sites. Right: with the 42 broadband sites.

6.2.4 Data and processing examples

6.2.4.1 Comparison of old and new sensors

After installation of the new hybrid instruments, several tests were performed to compare old and new data-processing results. During a transition period in autumn 2011, the KS54000 and the new NORSAR 360 s CMG-3T Hybrid instruments were co-located and recorded in parallel. Figure 6.2.10 shows beams of the vertical components (KS54000: BEAM-1, CMG-3T Hybrid: BEAM-2) for a surface wave in the long-period frequency range (15–30 s) from a M_s 4.4 earthquake in Turkey (29.10.2011, 22:24:22.9, 38.82N, 43.43E, depth: 0 km, distance: \sim 3250 km). The data for the seventh 3C site (NC602) were simulated from the old CMG-3T broadband sensor. The signal-to-noise ratio (SNR) is improved by a factor of about 1.6 for the new instrumentation.

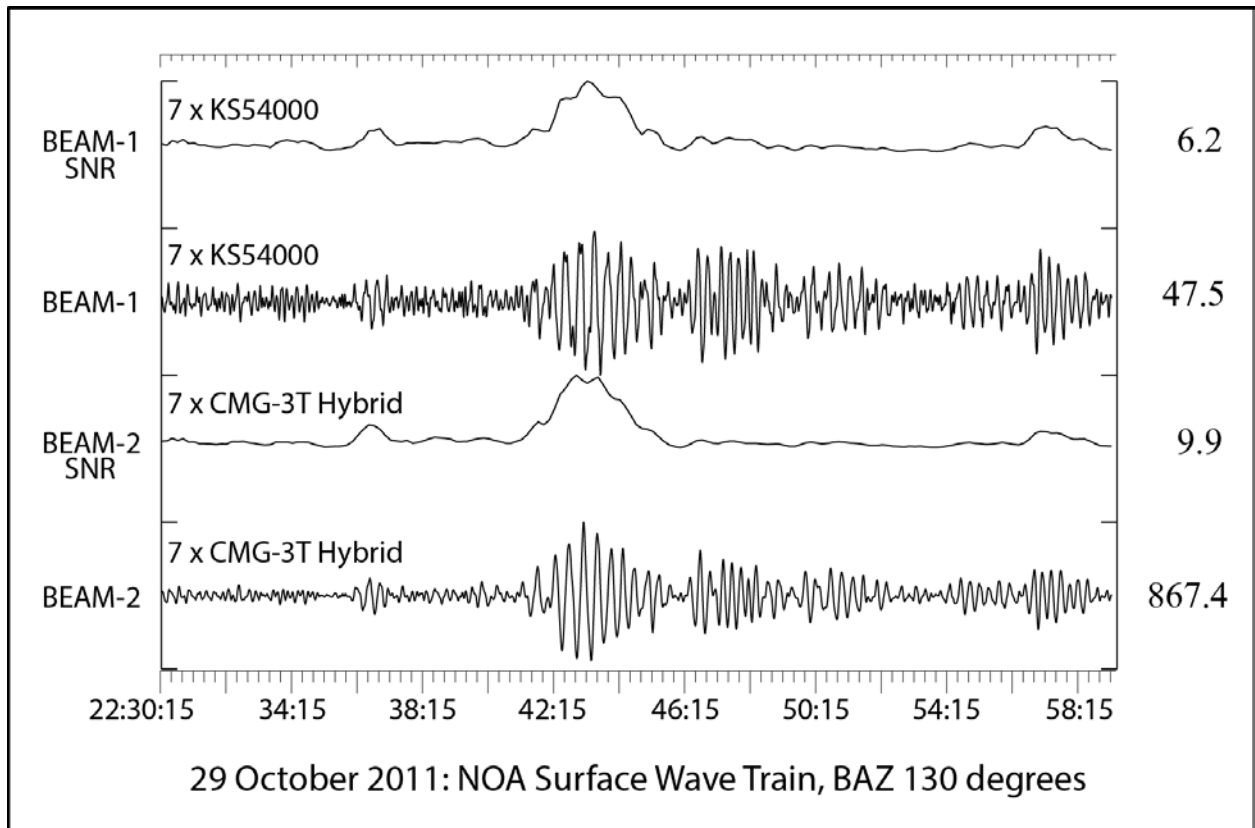


Fig. 6.2.10 Shown are the surface-wave beams calculated from the seven 3C instruments of NOA using the old (BEAM-1) and the new (BEAM-2) sensors and the corresponding SNR traces. The data were Butterworth bandpass filtered between 10 and 20s.

The frequency-wavenumber (fk) results for the seven vertical components of the same data are shown in Figure 6.2.11 (on the right: KS54000, on the left: CMG-3T Hybrid) and are very similar. However, comparing the size and amplitude of the two side lobes it is clear that they are a bit smaller and less pronounced for the new instrumentation. This improvement is due to the larger bandwidth of the new instrumentation.

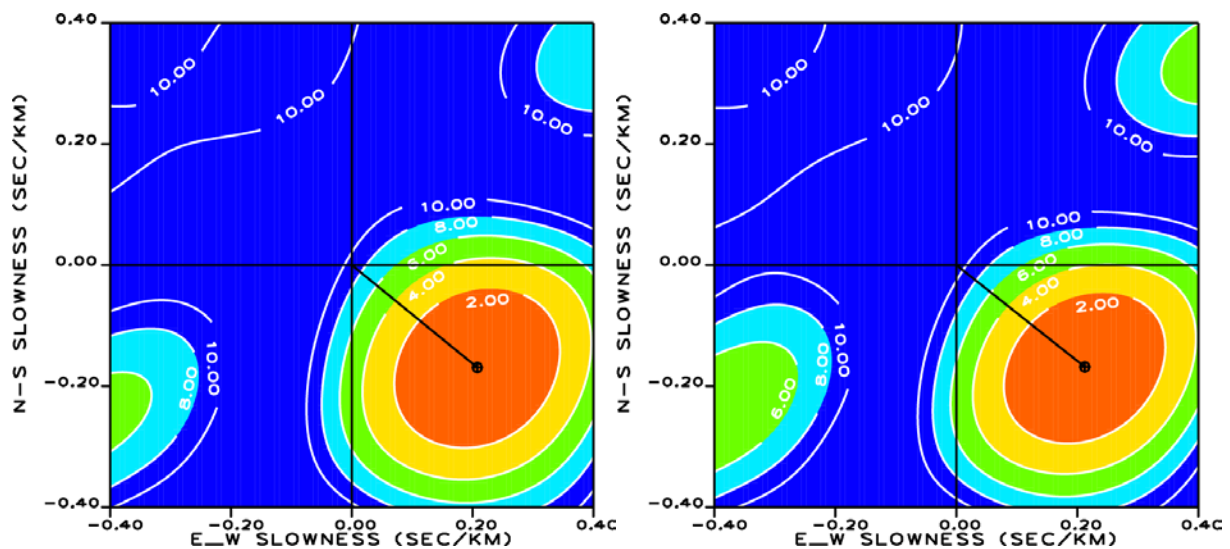


Fig. 6.2.11. Fk results for surface-wave trains of the 29 October 2011 event in Turkey, used were the seven vertical traces of the 3C sensors: the result for the seven KS54000 instruments are shown on the left and result for the seven new CMG-3T Hybrid sensors on the right.

6.2.5 Comparison of array configurations

After the whole array had been equipped with new CMG-3T Hybrid sensors, the array recorded surface waves generated by the 15 February 2013 Chelyabinsk Meteor impact (~3000 km distance). The LR phase is clearly visible on the records of all sites after bandpass filtering between 20 and 50 s (or 0.02 and 0.05 Hz). These data were used for the following study. Figure 6.2.12 shows as top trace (labelled NAO01s) an example for a single station recording the data of site NAO01 after simulating a KS54000 instrument. The third trace from top (labeled NAO01) shows the original CMG-3T Hybrid record. Although identically filtered these two traces already show the principle difference between the new and the old instrumentation: the new instrumentation has a higher sensitivity and the low frequency contents is larger. The other traces show beams calculated for different configurations. For BEAM-1 only the KS54000 simulated vertical traces of the 3C sites were used to simulate the old NOA surface wave capability, for BEAM-2, the unchanged CMG-3T Hybrid vertical traces of the 3C sites were used to show the improvement by the new instrumentation and finally for BEAM-3, the 40 available CMG-3T Hybrid vertical traces were used (two sites out of the 42 were down) to demonstrate the new NOA capabilities to observe and analyze seismic surface waves. The SNR improvement with the new instruments is significant as well as the larger dynamic range.

The fk-results for the three array configurations are shown in Figure 6.2.13. The results for the two 7 element arrays (for BEAM-1 on the left and for BEAM-2 in the middle) differ not much. This is in agreement with the above shown example (Figure 6.2.11). But the side-lobe suppression for the fk-analysis is significantly improved, when using the 40 available broadband elements of the new NORSAR array (for BEAM-3, on the right).

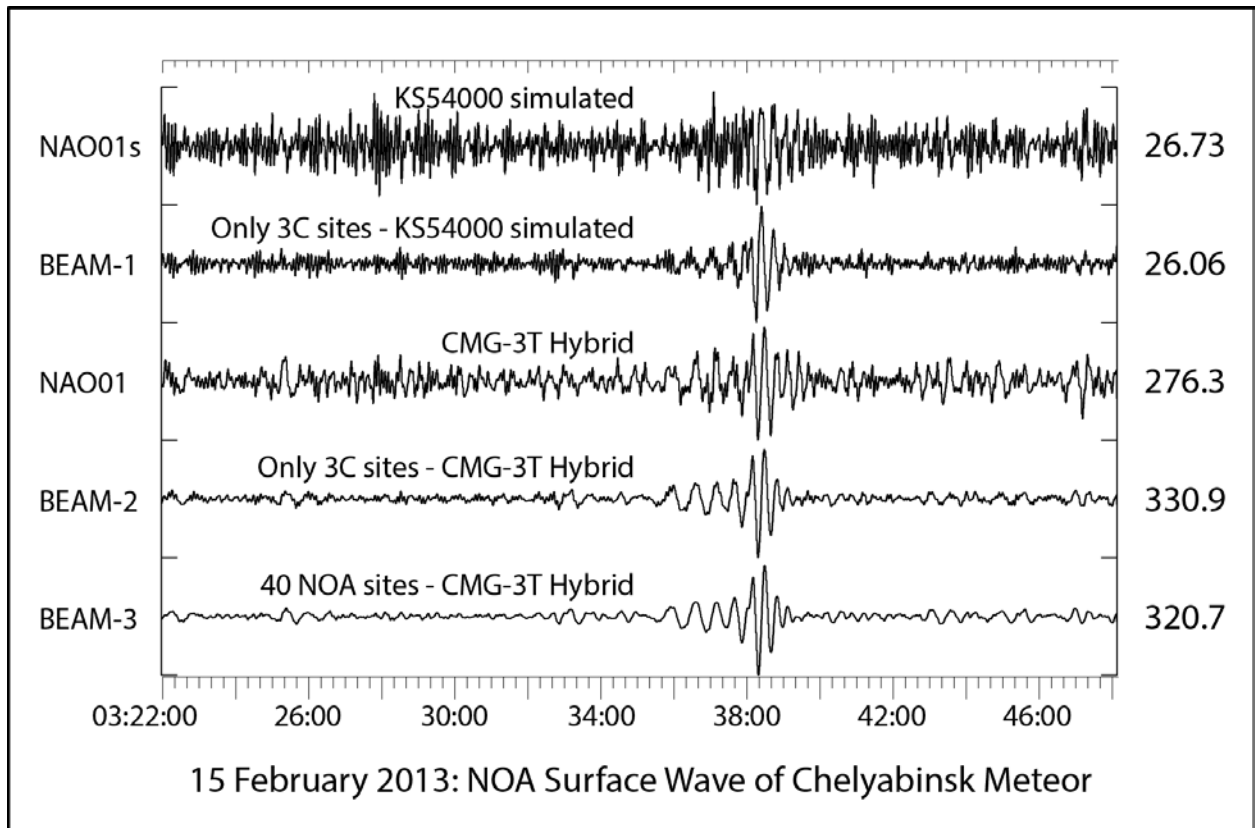


Fig. 6.2.12. The figure shows bandpass filtered (20 – 50 s) surface wave observations generated by the Chelyabinsk Meteor impact (~3000 km distance). The top trace (NAO01s) shows a KS54000 simulation for the recording at NOA site NAO01, the second trace (BEAM-1) shows a beam of the simulated KS54000 recordings from all the 7 sites with 3C instrumentation, corresponding to the old NORSAR array configuration. The middle trace (NAO01) shows the CMG-3T Hybrid recording at NORSAR array site NAO01. The lower two traces show array beams of the new NORSAR Hybrid instrumentation data; BEAM-2 for the 7 sites with 3C instrumentation and BEAM-3 for all 40 available NORSAR array elements.

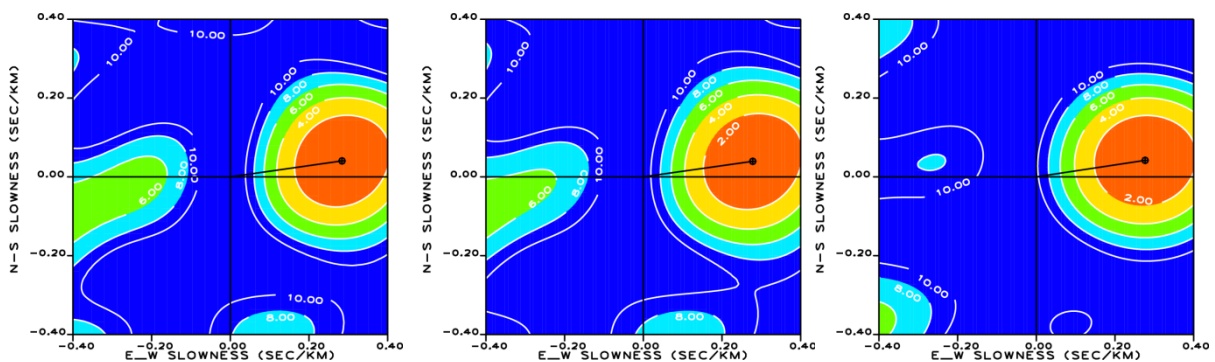


Fig. 6.2.13. Shown are the fk-analysis results for the three beam configurations of Figure 6.2.12. The results for the two 7 element arrays for BEAM-1 on the left and for BEAM-2 in the middle. The fk-analysis result for the 40 available broadband elements of the new NORSAR array (BEAM-3) is shown on the right.

6.2.6 Time corrections for the new NOA broadband array

Figure 6.2.14 shows, the vertical component recordings at the NOA site NB200 from two events in Iran (left: 16 April 2013, Mw 7.8; right: 12 May 2013, M 5.6), unfiltered (at the top) and filtered with different bandpass filters. It is obvious that the dominant frequency range varies for the different seismic phases. However, the smaller event cannot be observed at all frequencies.

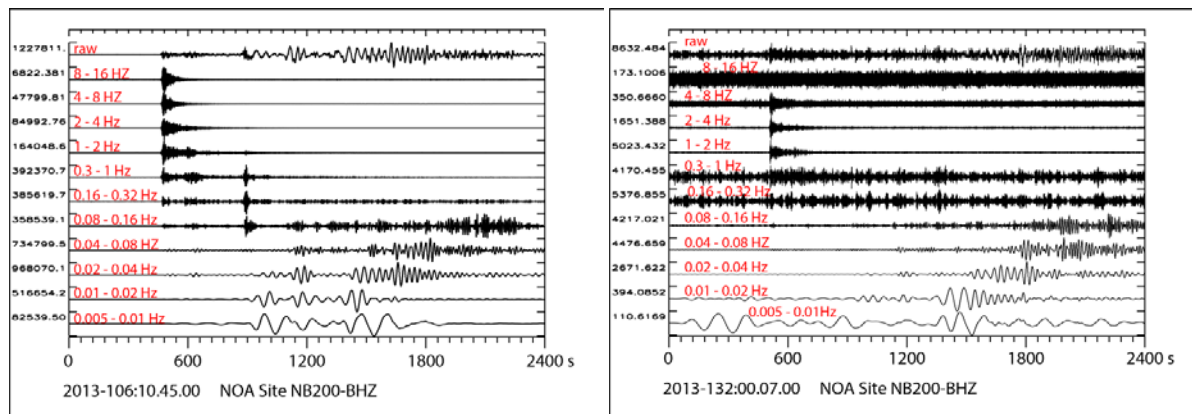


Fig. 6.2.14. Two earthquakes in Iran (left: 16 April 2013, 10:44:20 UTC, Mw 7.8; distance = 47.1°; right: 12 May 2013, 00:07:04 UTC, M 5.6; distance = 46.3°). All traces are normalized with their maximum amplitudes. The top traces are the raw data as recorded with the new CMG-3T Hybrid sensors. The other traces show in different frequency ranges Butterworth bandpass filtered data.

Fk-analysis results of the first P-wave onsets of these two earthquakes are shown in Figure 6.2.15 and the numerical values are listed in Table 6.2.3. The results shown for the 12 May 2013 event (Figure 6.2.15a and Figure 6.2.15b) show that application of the known time corrections improve the fk-analysis results in the typical frequency range of short period P waves: the data coherency becomes larger, the estimated backazimuth and apparent velocities are closer to the theoretically expected values and the number of side lobes is drastically reduced.

For the larger 16 April 2013 event the P-wave onset has significant amplitudes also at much lower frequencies (see Figure 6.2.14) and for the fk-analysis a much larger frequency range (here 0.08 – 4 Hz) can be utilized. The results are shown in Figures 6.2.15c and 6.2.15d. A comparison of the theoretical with the estimated values for backazimuth and apparent velocity show again a slight improvement after applying the time corrections, but the signal coherency decrease and the side lobes become more pronounced. This discrepancy can be explained as follows: The time corrections for NOA were developed for the large short-period NAO array in the 1970s. They empirically correct for lateral velocities below the array for signals with dominant frequencies between about 1 and 5 Hz. If it now becomes possible to analyze P-wave signals for much lower dominant frequencies (i.e., much larger wavelengths), the signals are dominantly influenced by lateral velocity heterogeneities in much larger volumes. In conclusion, the time corrections are signal frequency dependent and new empirical time corrections should be determined for utilizing the full possible frequency range for array studies.

Table 6.2.3: Fk-analysis results for the two Iran events.

Event	Figure	Frequency Band [Hz]	Backazimuth [deg]		App. Velocity [km/s]		Signal Coherence	Time Corrected
			Theory	Observed	Theory	Observed		
12/05/2013	15 a	1 – 4	116.77	118.01	14.15	13.76	0.26	no
12/05/2013	15 b	1 – 4	116.77	115.01	14.15	14.19	0.51	yes
16/04/2013	15 c	0.08 – 4	110.68	114.82	14.29	14.62	0.43	no
16/04/2013	15 d	0.08 – 4	110.68	108.34	14.29	14.60	0.38	yes

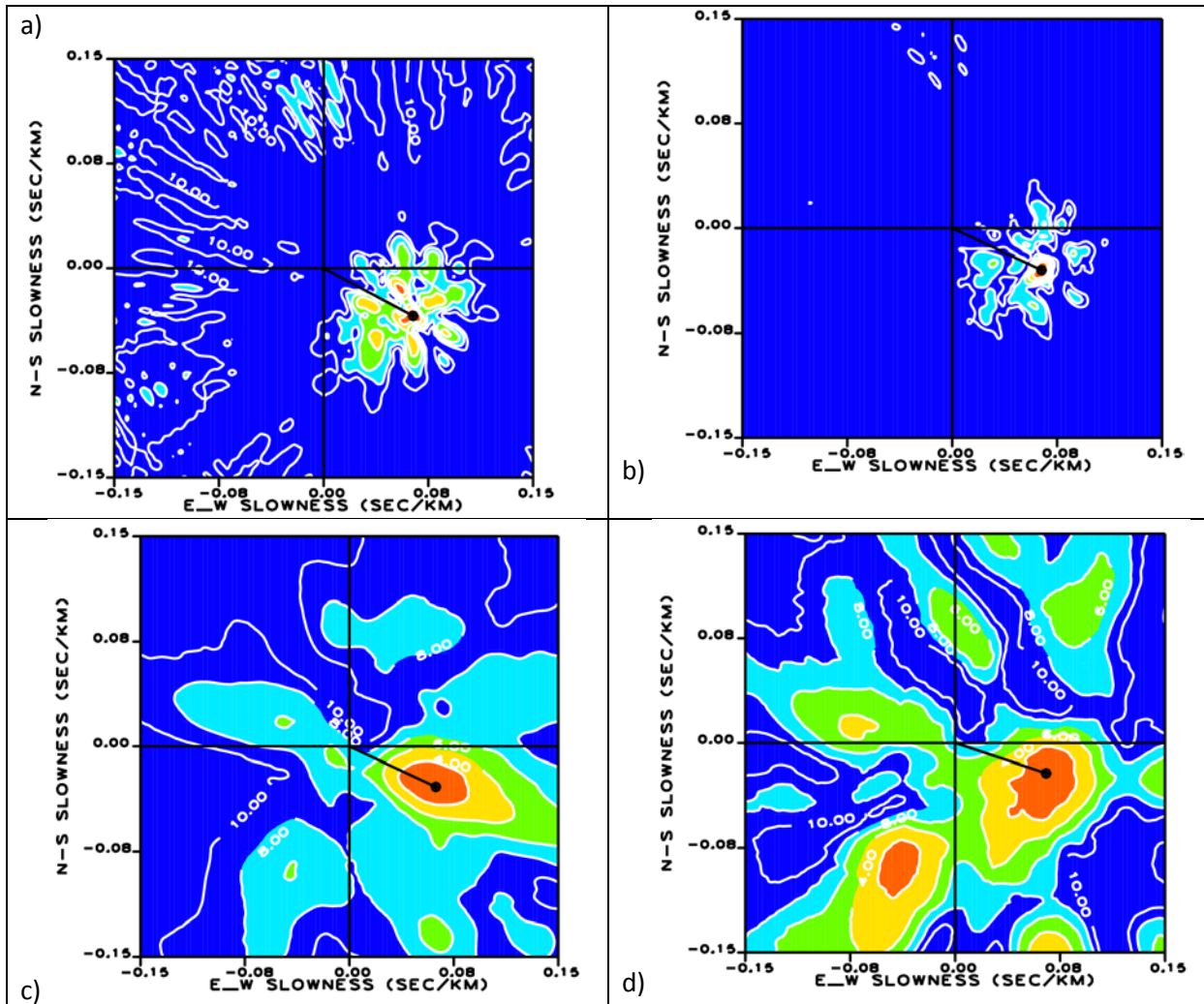


Fig. 6.2.15. Fk-analysis results for the two Iranian earthquakes: a) and b) for the 12 May 2013 event and c) and d) for the 16 April 2013 event. NOA time corrections were applied for the results on the right (b and d).

M. Roth
 J. Schweitzer
 J. Fyen

References

Pirli, M. (2013). NORSAR System responses manual, 3rd Edition, NORSAR, 304 pp. + 5 Appendices.

Roth, M., J. Fyen, P. W. Larsen and J. Schweitzer (2011). Test of new hybrid seismometers at NORSAR, NORSAR Sci. Rep. **1-2011**, 61-71.